



ISSN 0975-413X  
CODEN (USA): PCHHAX

Der Pharma Chemica, 2016, 8(4):418-424  
(<http://derpharmachemica.com/archive.html>)

## CFD Photochemical Modelling in an Urban Street Canyon

Merah Aissa<sup>1,2\*</sup>, Noureddine Abdelkader<sup>2</sup> and Abidat Miloud<sup>2</sup>

<sup>1</sup>Centre de Recherche Scientifique et Technique en Analyses Physico-Chimiques, BP 384, Siège ex-Pasna Zone Industrielle, Bou-Ismaïl CP 42004, Tipaza, Algérie

<sup>2</sup>Laboratoire de mécanique appliquée LMA, Université des sciences et de la technologie d'Oran Mohamed BOUDIAF (USTO-MB), Algérie

---

### ABSTRACT

The nitrogen oxide gases are subject to fast chemical reactions. The time scales characterizing these reactions are of the order of tens of seconds and thus, comparable with residence time of pollutants in street canyons. The objective of the present study is the performance of small-scale computations for an urban 3D by using a CFD (computational fluid dynamics) code (ANSYS-CFX) to provide steady state wind and pollutant concentration fields. A fast chemistry module simulating chemical reactions taking place within street canyons right after traffic pollutants are emitted is implemented to the model in order to assess the concentrations of NO<sub>x</sub> and ozone in space. Circulations created by the city itself and that affect pollutant dispersion are accounted for and hotspot concentrations that depend on street canyon scale effects are also computed. Reactive pollutant dispersion in the street canyon has been numerically investigated using CFD numerical simulation by means of k-ε turbulence model and transport equations for NO, NO<sub>2</sub>, and O<sub>3</sub> with simple photochemistry. The area emission source is divided to sub-domains describing NO<sub>x</sub> vehicles' emissions. The Background of O<sub>3</sub> was specified, and the gases were allowed to mix and react.

**Keywords:** Street canyon; Photochemistry; Computational fluid dynamics (CFD); O<sub>3</sub>; NO<sub>x</sub>.

---

### INTRODUCTION

The study on flow and dispersion in urban street canyons have been widely investigate and attracted great concern during the past two decades mainly due to increasing urban pollutants and their adverse impacts on human health. Field measurements and computational fluid dynamics (CFD) techniques are the common tools used to study the flow and pollutants dispersion in street canyons.

The CFD modeling approach as a way to understand street canyon flow and dispersion has become powerful and comprehensive with recent advances in computing power, numerical method/algorithm, and turbulence parameterization. Previous CFD modeling studies have contributed to our understanding of the many important aspects of street canyon flow and dispersion. These include flow regime, dispersion mechanism [2], thermal effects on flow and dispersion [4].

In urban areas, a main pollutant source is automobiles and the pollutants emitted from automobiles, for example NO and NO<sub>2</sub>, are chemically reactive. Complex photochemical processes in densely built-up urban areas with traffic often result in a serious air pollution problem. Therefore, to further enhance our understanding of street canyon dispersion, reactive pollutants need to be taken into account.

## MATERIALS AND METHODS

### 2.1. Selected case and simulation

Due to rapid growth of traffic volumes within urban areas, pollutant concentrations are still receiving a lot of attention in densely built-up areas where people are concentrated and where both buildings and the people are more affected.

The street simulated in CFX, is One-way Street, the Width of the street varies with an average value of 10m and with a length of 95m. This street has about 19 building with heights varying between 3m and 18m.

#### 2.1.1. Emission of cars

Traffic emissions in the street are calculated knowing the traffic flow (vehicle/hour) and emission factors (g/km). The basic formula for estimating emissions, using experimentally (The Core Inventory of Air Emissions in Europe CORINAIR, 3<sup>rd</sup> Edition 2003 [6]) obtained emission factor is:

Emissions per Period of Time [g] = Emission Factor [g/km] × Number of Vehicles [veh.] × Mileage per Vehicle per Period of Time [km/veh.]

The emissions factor depends the vehicle speed (for NO<sub>x</sub>), with engine capacity CC < 1.4 l given as:

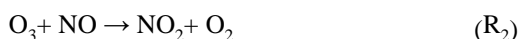
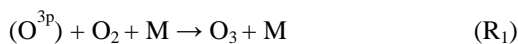
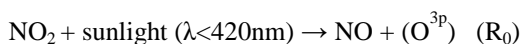
$$E = 0.5595 - 0.01047V + 10.8e^{-5}V^2 \text{ [g/km].}$$

Where V is the vehicle speed.

#### 2.1.2. Chemical coupling of O<sub>3</sub>, NO, and NO<sub>2</sub>

The reactive pollutants we are concerned with in this study are nitrogen oxide NO and nitrogen dioxide NO<sub>2</sub>, which are supposed to be emitted from automobiles within the street canyon in the presence of background ozone O<sub>3</sub>.

The chemical reactions considered are:



M represents a molecule (N<sub>2</sub> or O<sub>2</sub> or another third molecule).

#### 2.1.3. Reaction rate type

Chemical kinetics characterizes the rate at which chemical species appear or disappear. The kinetic rate constant (of reaction) is a function of temperature and is given in the form:

$$k(T) = AT^\beta \exp\left(\frac{-E_a}{RT}\right) \quad (1)$$

This equation is called the Arrhenius equation (used by ANSYS CFX), where A is a pre-exponential factor,  $\beta$  is the temperature exponent, R is the universal gas constant, T is the temperature, and E<sub>a</sub> is the activation energy.

#### 2.1.4. Model description

Computational fluid dynamics (CFD) modelling is based on the governing fluid flow and dispersion equations, which are derived from basic conservation and transport principle:

- The mass conservation (continuity) equation.
- The three momentum (Navier-Stokes) equations in x, y, z.
- The transport equation for pollution concentration.

The air within the street canyon can be regarded as an incompressible turbulent flow, and the air and pollutants densities are assumed to be constant. These assumptions are reasonable for lower atmosphere environment as described by Sini et al., 1996 [4].

For the street canyon problem, the standard  $k$ - $\varepsilon$  turbulence model governing equations expressed as:

The continuity equation:

$$\frac{\partial U_i}{\partial x_i} = 0 \quad (2)$$

The momentum equation:

$$\frac{\partial U_i}{\partial t} + U_j \frac{\partial U_i}{\partial x_j} = -\frac{1}{\rho} \frac{\partial \bar{p}}{\partial x_i} + \frac{\partial}{\partial x_j} \left( \nu \frac{\partial U_i}{\partial x_j} - \overline{u'_i u'_j} \right) \quad (3)$$

$k$  and  $\varepsilon$  transport equations in the standard  $k$ - $\varepsilon$  model:

$$\frac{\partial k}{\partial t} + \vec{V} \text{grad} k = \text{div} \left( \frac{\nu_t}{\sigma_k} \text{grad} k \right) + P - \varepsilon \quad (4)$$

$$\frac{\partial \varepsilon}{\partial t} + \vec{V} \text{grad} \varepsilon = \text{div} \left( \frac{\nu_t}{\sigma_\varepsilon} \text{grad} \varepsilon \right) + \frac{\varepsilon}{k} (C_{\varepsilon_1} P - C_{\varepsilon_2} \varepsilon) \quad (5)$$

$k$ : turbulent kinetic energy;  $\varepsilon$ : turbulent dissipation rate.

Where:

$$\nu_t = C_\mu \frac{k^2}{\varepsilon}; \quad \overline{u'_i u'_j} = -2\nu_t S_{ij} + \frac{2}{3} k \delta_{ij}; \quad P = 2\nu_t S_{ij} S_{ij}; \quad S_{ij} = \frac{1}{2} \left[ \frac{\partial U_i}{\partial x_j} + \frac{\partial U_j}{\partial x_i} \right]$$

Table 1: The constants for  $k$ - $\varepsilon$  turbulence model

$C_\mu$	$\sigma_k$	$\sigma_\varepsilon$	$C_{\varepsilon_1}$	$C_{\varepsilon_2}$
0.09	1	1.3	1.44	1.92

Pollutant concentration is calculated with the convective-diffusion equation:

$$\frac{\partial C_i}{\partial t} + U_j \frac{\partial C_i}{\partial x_j} = \frac{\partial}{\partial x_j} \left( K_i \frac{\partial C_i}{\partial x_j} \right) + S_i \quad (6)$$

Where  $C_i$  denotes the pollutant concentration,  $K_i$  is the eddy diffusivity coefficient; and  $S_i$  represents all sources and sinks terms.

### 2.1.5. Computational domain

The Figure 1 illustrates the computational domain, and building configuration. This study models reactive pollutant dispersion in a long street when the wind direction ( $x$ -direction) is parallel to the street direction. The origin of the coordinate system is located at the left bottom corner of the street in the computational domain. The domain size is 95m in the  $x$ -direction, 16m in the  $y$ -direction, 21m in  $z$ -direction.

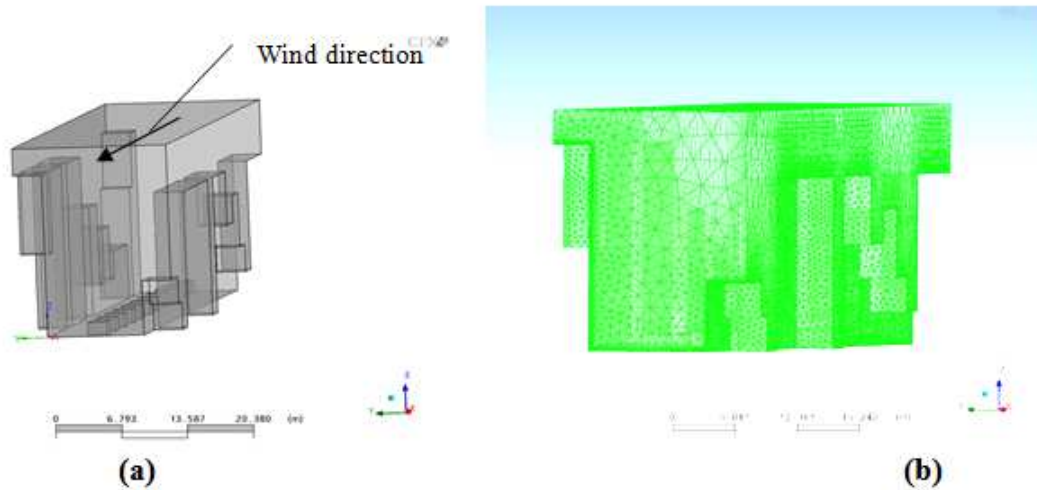


Figure 1. a) Computational domain and buildings configuration  
 b) Mesh of the complete computation domain.

2.2. Initialization

The emission sources considered in this study are sub-domains (volume sources), created along the street in x-direction (11 sub-domains or cars), with size of 3.5m×2m×1.48m (each car), and the distance between two cars is 5m. The vehicles were assumed to emit NO (90% of NO<sub>x</sub>), NO<sub>2</sub> (10% of NO<sub>x</sub>). We estimate the emission rate for each car, as NO emission rate of 16.5 μg/m<sup>3</sup>s, and 2.5 μg/m<sup>3</sup>s of NO<sub>2</sub>. A background ozone concentration of 70μg/m<sup>3</sup> was then set for the entire domain [5], [3]. At the inflow boundary, wind assumed to blow along the canyon the street from east to west; with a speed of 1.5 m/s. The pressure and temperature were specified as 1 atm and 25<sup>0</sup>C, respectively.

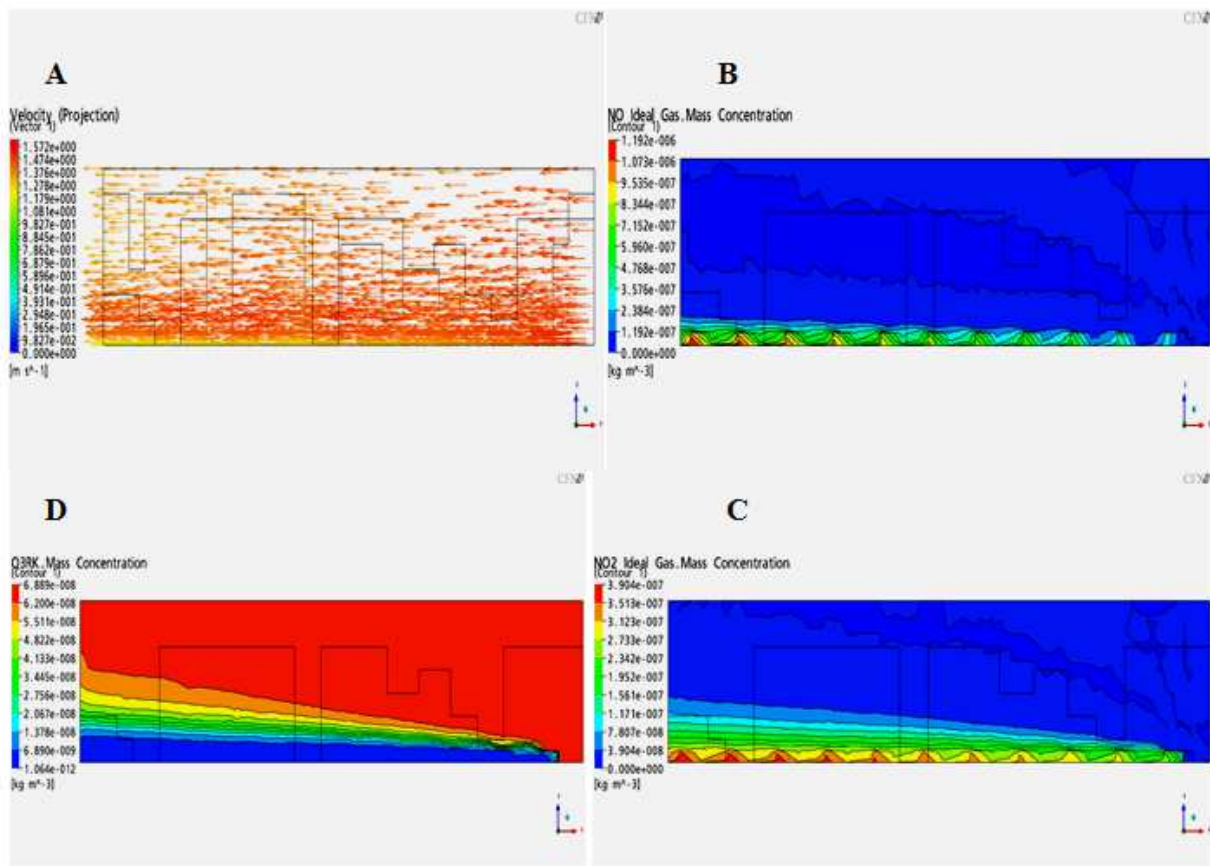


Figure 2. A) velocity vectors; B) NO, C) NO<sub>2</sub>, and D) O<sub>3</sub> concentration contours on x-z plane at y=-5m (middle of street)

## RESULTS AND DISCUSSION

As shown in Figure 2 the effect of wind direction was crucial and a key factor determining the dispersion of pollutants. It was very interesting to see how the concentration distribution is behaving with respect to the flow field.

Wind parallel to the street direction resulted in higher  $O_3$  concentration levels in the middle upper area of the street (Fig.2.D). The accumulation of pollutants ( $NO$ ,  $NO_2$ ) along the canyon axis dominates close to the vehicular emission sources (Fig.2.B and Fig.2.C). Ozone ( $O_3$ ) concentration is high apart from the upper region of the street and at inlet. This is explained by ozone rich air aloft being entrained into the canyon, followed by dispersion and reaction. A very interesting symmetric level has been occurred between ozone  $O_3$  and  $NO_2$  that follow opposite trends [7]. A steady rise in ozone level was observed with decreased  $NO_2$  concentration.

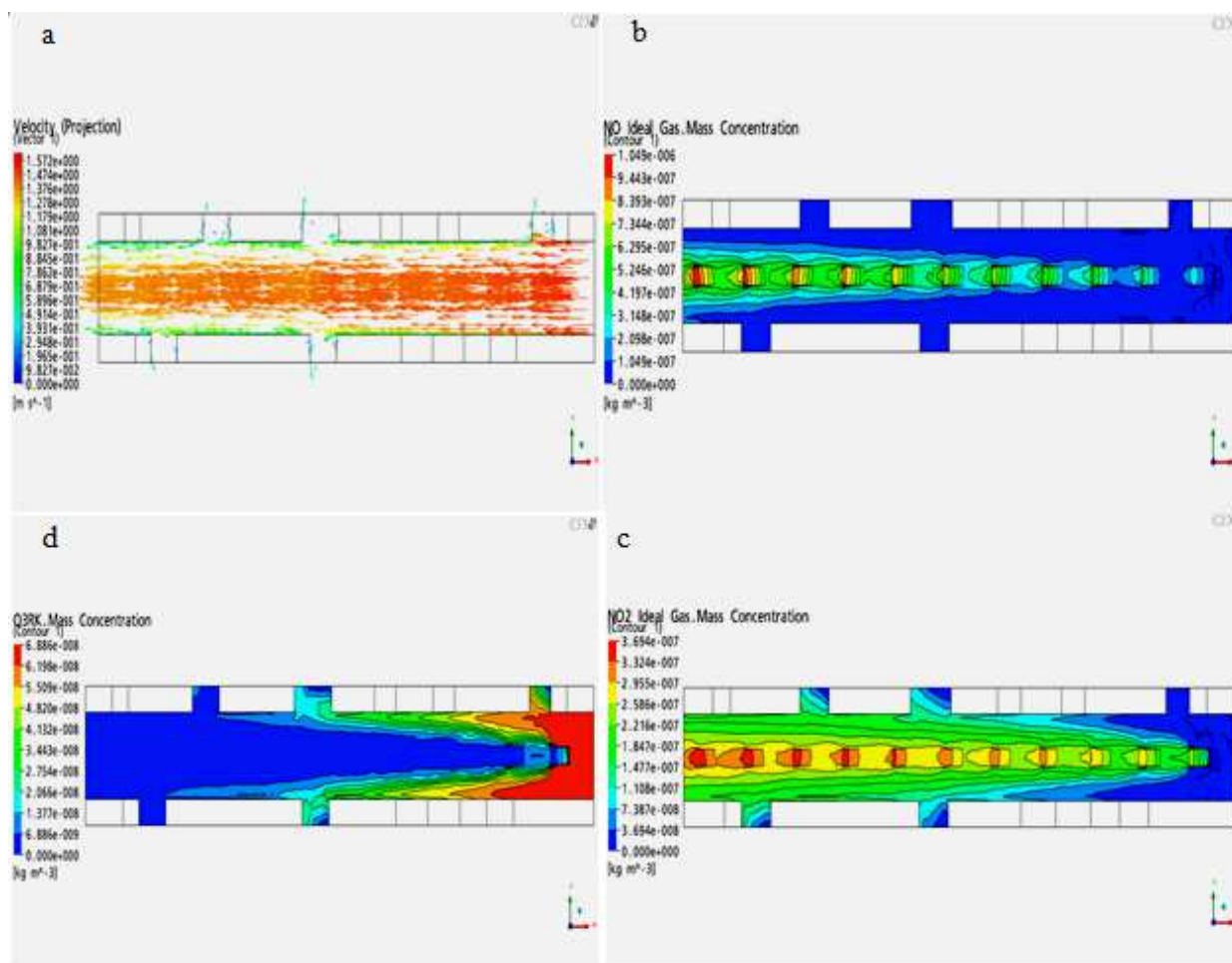
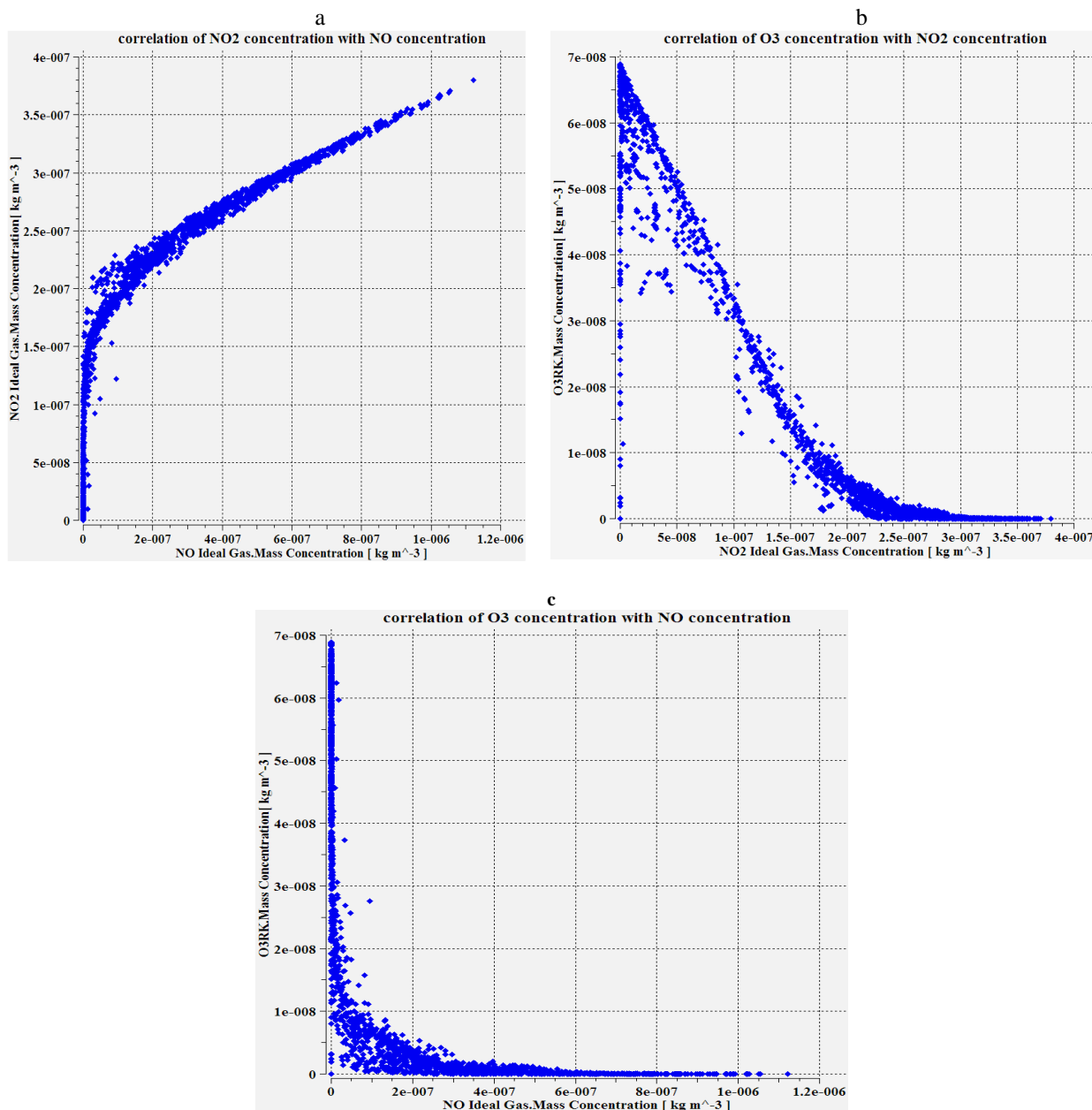


Figure 3. a) velocity vectors; b)  $NO$  concentration, c)  $NO_2$  concentration, and d)  $O_3$  Concentration contours on x-y plane at level  $z = 1m$  (near the ground)

It is illustrated clearly that concentration of  $NO$  and  $NO_2$  in the areas near the emission source-traffic road (Figure 3.b. and Figure 3.c), are significantly higher than that of any other areas and very low close to the buildings. The spatial distribution of  $NO_2$  is larger than  $NO$ , because  $NO$  is quickly transformed to  $NO_2$ . Furthermore the concentration of  $NO$  and  $NO_2$  are much lower in the inflow region than the rest of the canyon. This is in contrast with  $O_3$  that is high at the inlet. This is explained by the consumption of ozone  $O_3$  by  $NO$  in the street canyon to varying degrees. And the flow speed in the left side (Figure 3.a) near the ground level is weak and hence the pollutants have sufficient time spent in the mixing and reaction process of the chemical species [1]. On the other hand, there is a formation of  $NO_2$  due to the reactions between  $O_3$  and  $NO$  and thus,  $NO_2$  dispersed more significantly than  $NO$ . As expected,  $NO$  and  $NO_2$  concentration levels decrease with height while that of ozone generally increases.



**Figure 4. Domain average concentration correlation:**  
 a)- correlation of NO<sub>2</sub> concentration with NO concentration.  
 b)- correlation of O<sub>3</sub> concentration with NO<sub>2</sub> concentration.  
 c)- correlation of O<sub>3</sub> concentration with NO concentration.

Figure 4.a shows the correlation of NO<sub>2</sub> concentration with NO concentration. The increasing NO<sub>2</sub> concentration with increasing NO concentration is displayed this variation is approximately linear above  $1.5 \times 10^{-7} \text{ kg/m}^3$  of NO<sub>2</sub> concentration, until the maximum values of NO and NO<sub>2</sub> concentrations, which are  $\sim 1.19 \times 10^{-6}$  and  $\sim 3.9 \times 10^{-7} \text{ kg/m}^3$ , respectively. This case reflects the high concentration levels of NO and NO<sub>2</sub> near the ground, where their emission source is located. Note that the values of NO concentration is greater than NO<sub>2</sub> concentration, due to the rate of emission source that was assumed with a ratio one-tenth (1/10), of NO<sub>2</sub> to NO.

Except in the region below  $1.5 \times 10^{-7} \text{ kg/m}^3$  where NO<sub>2</sub> concentration varied between zero to  $1.5 \times 10^{-7} \text{ kg/m}^3$  with nearly zero NO. This was because NO<sub>2</sub> dispersed more than NO corresponding to areas at high levels. Because NO is quickly transformed to NO<sub>2</sub> (Figure 2.C and Figure 3.c).

The corresponding NO<sub>2</sub> and O<sub>3</sub> concentration levels are displayed in Figure 4.b, that shows decreasing O<sub>3</sub> concentration with increasing NO<sub>2</sub> concentration. This indicates the oxidation of NO by ozone O<sub>3</sub> that leads to an increase in the NO<sub>2</sub> concentration and linear decrease of ozone levels.

It is interesting in Figure 4.c to observe the difference between NO and O<sub>3</sub> concentrations. As it shown the increase of NO concentration (for  $2 \times 10^{-7} \text{kg/m}^3$  until a maximum value) with low O<sub>3</sub> concentration, implies that the ozone O<sub>3</sub> is consumed in high degree by NO due to the reaction with it near the emission source region.

A similar behaviour is observed for O<sub>3</sub> concentration (more than  $10^{-8} \text{kg/m}^3$ ) with low NO. Because O<sub>3</sub> concentration is high in the upper region of the street and in the inlet boundary. NO concentration was negligible in these regions. In addition there are some areas (Figure 4.c) where low O<sub>3</sub> concentration (less than  $10^{-8} \text{kg/m}^3$ ), the NO concentration was low too (less than  $2 \times 10^{-7} \text{kg/m}^3$ ). This result corresponds to areas close to building surfaces, where O<sub>3</sub> and NO were both considerably low, due to low wind speed and weak dispersion ability of NO. Also note that NO<sub>2</sub> concentration is low in these areas (Figure 2).

### CONCLUSION

This study examined reactive pollutant dispersion in 3D urban street canyon in steady state. A CFD (computational fluid dynamics) code was used (ANSYS-CFX), with a standard k-ε turbulence model using transport equations for the mean concentration and concentration variance of the scalars, incorporating simple NO-NO<sub>2</sub>-O<sub>3</sub> photochemistry. An area emission source of NO and NO<sub>2</sub> was considered in the presence of background O<sub>3</sub>.

- The study also shows evidence that the reactive gases considered were NO and NO<sub>2</sub> emitted into the canyon by traffic against a background of ozone. This implied that Background ozone, transported into the canyon from inflow region (inlet), is destroyed by the NO emissions from the motor vehicles, in particular at low levels.
- The fast reaction of the emitted NO with O<sub>3</sub> leads to the high NO<sub>2</sub> concentration (because NO is quickly transformed to NO<sub>2</sub>). In addition we observed that NO<sub>2</sub> dispersed more significantly than NO to higher levels, probably because it comes from both primary combustion sources within the street Canyon (direct emission from cars) and secondary formation from the NO+O<sub>3</sub> reaction. As a result O<sub>3</sub> concentration is higher at upper levels and in the region where ambient O<sub>3</sub> enters into the canyon, while NO and NO<sub>2</sub> are depleted in a high degree in these areas (Figure 2).
- The highest ozone O<sub>3</sub> concentration occurred under high wind speeds; the wind speed dependency becomes more distinct in Figure 2. The results indicated that there is a strong influence of the street geometry on the wind field and consequently the pollutant dispersion around the buildings surfaces.

### REFERENCES

- [1] Baik Jong-Jin, Kang Yoon-So, Kim Jae-Jin, **2007**, *Atmospheric Environment* 41, 934–949.
- [2] Baik Jong-Jin, Kim Jae-Jin, **2002**, *Atmospheric Environment* 36, 527–536.
- [3] Baker Jacob, Walker Helen L., Cai Xiaoming, **2004**, *Atmospheric Environment* 38, 6883–6892.
- [4] J. F. Sini, S. Anquetin, G. Mestayer, **1996**, *Atmospheric Environment* 30, 2659–2677.
- [5] R. Stern, R.J. Yamartino, **2001**, *Atmospheric Environment* 35, 149-165.
- [6] The Core Inventory of Air Emissions in Europe, CORINAIR, third Edition **2003**. Group 7, Road Transport.
- [7] A.G. Triantafyllou, S. Zoras, V. Evagelopoulos, S. Garas, C. Diamantopoulos, **2008**, *Global NEST Journal*, Vol 10, No 2, pp 161-168.